

TEMPORAL VARIATIONS OF FRACTURE DIRECTIONS AND FRACTURE DENSITIES IN THE COSO GEOTHERMAL FIELD FROM ANALYSES OF SHEAR-WAVE SPLITTING

Gordana Vlahovic, Maya Elkibbi and Jose A. Rial

Wave Propagation Laboratory
Department of Geological Sciences
University of North Carolina at Chapel Hill, NC 27599-3315
vlahovic@email.unc.edu

ABSTRACT

This project aims to improve understanding of the subsurface fracture system in the Coso geothermal field, located in the east central California. We applied shear-wave splitting technique on a set of high quality, locally recorded microearthquake (MEQ) data. Four major fracture directions have been identified from the seismograms recorded by the permanent sixteen-station down-hole array: N10-20W, NS, N20E, and N40-45E, of which the first and the third are the most prominent. All orientations are consistent with the known strike of local sets of faults and fractures at depth and at the surface, as well as with previous analyses of seismic anisotropy in the region. Significant changes in shear-wave time delays, which are governed by crack density, have been detected from data recorded during five consecutive years (1996-2000). Variations in shear-wave time delays were simulated using synthetic seismograms and tentatively interpreted as due to a local ~3% decrease in shear-wave anisotropy in the southwestern part of the field during 1999.

INTRODUCTION

The Coso geothermal field is located along the eastern front of the Sierra Nevada, in the southwestern Basin and Range Province, California. Tectonics of the Coso range is the reflection of stress field that is influenced by both, the right slip San Andreas Fault system and the extensional Basin and Range environment (Roquemore, 1980). With an average of more than 20 MEQ's per day, the Coso area is one of the most active seismic regions of southern California. Most of the events below the field itself are less than 3 km deep and are surrounded by deeper regional seismicity (down to 12 km depth). Shallower hypocenters within the geothermal field and spatial overlap of microseismicity with geothermal borehole locations suggest association between seismicity and production activities (Feng and Lees, 1998). Since 1990, the microseismic activity at the field has been

monitored by the Coso Digital Downhole Seismic Network (CDDSN), which is composed of 16 three-component seismic stations (Fig. 1) recording at 480 samples/sec. The uninterrupted operation of the seismic network during the last six years resulted in the collection of a dataset of MEQ recordings of exceptional richness and continuity.

SHEAR-WAVE SPLITTING ANALYSIS

The analysis of split shear waves from microearthquakes has been shown to be a valuable technique to detect the main orientation and intensity of fracturing in the subsurface of geothermal fields (e.g., Lou and Rial, 1997). The method is based on the fact that a shear-wave propagating through rocks with stress-aligned, fluid filled cracks will split into two waves, a fast one polarized parallel to the predominant crack direction, and a slow one, polarized perpendicular to it (Crampin, 1981).

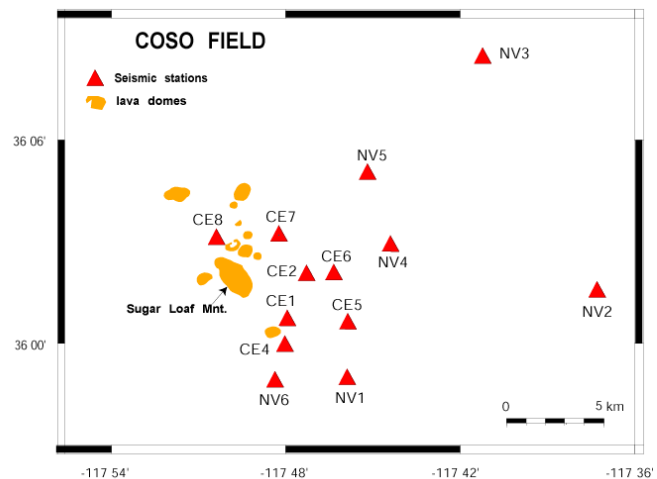


Figure 1. Coso Digital Downhole Seismic Network (CDDSN). Stations W1S and W2S are not shown. Lava domes and Sugar Loaf Mountain shown for reference.

The time delay between the fast and the slow wave is proportional to crack density, or number of cracks per

unit volume (Hudson, 1981). We shall designate the resulting fast wave polarization direction as ϕ and the time delay between the fast and the slow wave as δ . These are the two basic parameters measured from the split shear-wave seismogram.

During routine operation ϕ is measured by interactive rotation of the seismogram until the horizontal particle motion plot shows that fast and slow shear-waves are oriented along the instrument's horizontal components. Angle of rotation from the original polarization direction determines ϕ . At the same time, the two shear wave arrivals, which are generally coupled in the original recording, separate out in time domain and δ can then be readily measured by cross-correlation, or directly.

Such processing and analyses of over 10,000 microseismic events at the Coso geothermal field has resulted in substantial number of events per station displaying large signal to noise ratio, clear shear wave splitting, and arrival angles within the shear wave window. The latter is defined by the critical angle $i_c = \sin^{-1}(\beta/\alpha)$, where α and β are the P-wave and S-wave surface velocities respectively. The calculated i_c for the Coso geothermal area is approximately 35° , consequently, stations located on top of seismically active volume provide large numbers of reliable data, but stations relatively far (incident angle is 35° or more) from the same active centers provide only few reliable seismograms. Such is the case for some of the Navy stations, particularly NV4, NV5 and NV6 and station CE7. On the other hand, most of the other stations have provided large data sets with robust statistics, enough to accurately detect predominant fracture directions and delay times. The number of high quality data is generally large, so that even quality A data alone may provide robust statistics (quality A means high signal-to-noise ratio, sharply emergent S-wave, and delay times accurate to ± 2.08 ms). Fig. 2 shows the representative waveforms and observed splitting for the event inside the shear-wave window of the station CE6.

RESULTS

Crack orientations

The polarization orientations ϕ of the leading split shear-waves recorded within the shear wave window have been plotted in rose diagrams at each station of the array (Fig. 3). These orientations are assumed to mimic the predominant strike orientations of the subsurface local fracture system in the neighborhood of the recording seismic station (Crampin, 1981).

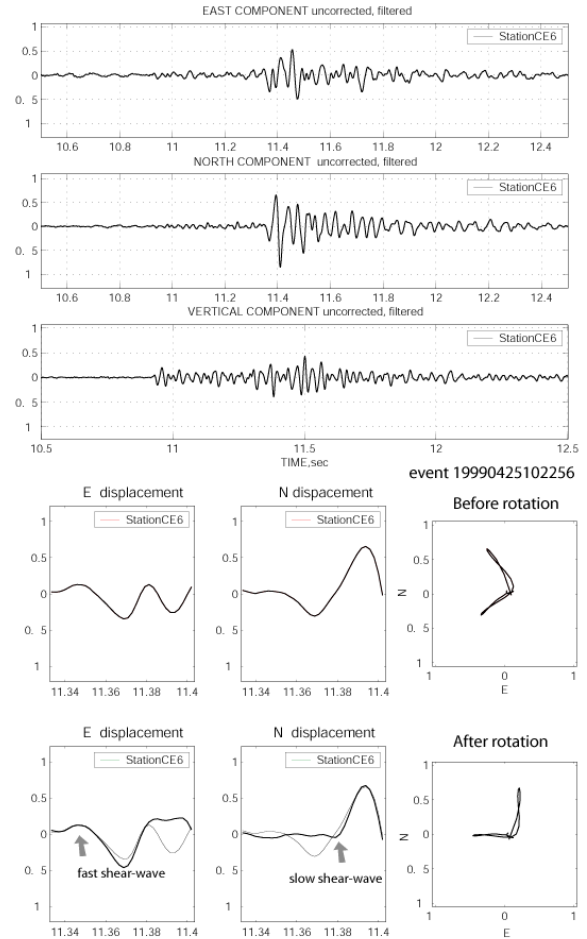


Figure 2. (top) Seismogram of the event 19990425102256, recorded at station CE6. (bottom) Seismogram is rotated 40° counterclockwise from the apparent E direction (in the down-hole instrument frame). After correction for instrument orientation, direction of the fast shear wave is N15W. Slow shear wave is 24 ms late.

As shown in Fig. 3, four major fast wave polarization directions have been identified at the Coso array: N10-20W, N-S, N20E, and N40-45E, of which first and third are the most prominent. These orientations are consistent with the strike of local sets of faults and fractures extending to the surface (e.g., Duffield and Bacon, 1981). Moreover, fractures measured by Schlumberger (M. Hasting, pers. comm., 2000) at various depth intervals in boreholes in the vicinity of stations CE1 and CE2, strike parallel to the directions of polarization obtained by shear wave splitting analysis, usually within five degrees.

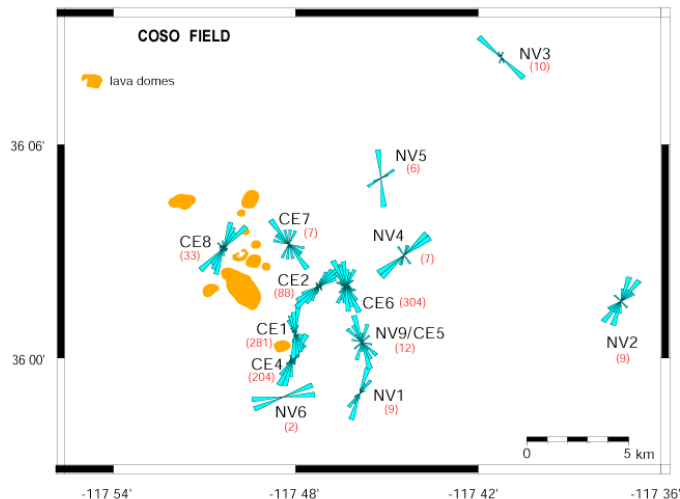


Figure 3. Fast shear wave polarizations observed at the Coso array. The figures in parenthesis refer to the number of determined polarizations used for each rose diagram. The data include all polarization readings of quality A through C collected during the first six months of the year 2000.

Although orientation of fast axis at some stations agree with the general NNE-SSW direction of maximum compressive stress (for example, stations CE2 and CE4), several stations have orientations of fast axis oblique to the direction of maximum compressive stress. Orientation of fast axis parallel to the fault-related paleo-fractures, such as at station CE6, can be explained by the high pore-fluid pressure that opened cracks oblique to the maximum horizontal stress (Angerer et al., 2000). With exception of stations with less than 10 data points, our polarization directions are consistent with earlier shear-wave splitting results from data collected before 1995 and analyzed by Lou and Rial (1994, 1997). Major polarization directions also agree with the results of P-wave anisotropy inversion by Lees and Wu (1999), who found that overall P-wave anisotropy is north-south fast in the western part and east-west fast in the eastern part of the Coso region.

Time delays

At Coso, time delay δt between the fast and slow split shear waves ranges between 10 and 50 milliseconds, so that the two shear-wave arrivals are usually well separated and their perpendicularity is clear. Since the sampling interval (2.08 ms) is nearly ten times shorter than the mean δt value (~ 20 ms) many measurements are highly reliable. Although a low-frequency source time function may affect the reading of short time delays, most events are within the same magnitude range, and source spectra are fairly constant in frequency content. In addition,

events are read for many azimuths and focal depths, so that the few inconsistent measurements are easily identified. In this work, δt is normalized by dividing it by the length L of the ray path. Since typically path lengths vary between 1 and 3 km, $\delta t/L$ ranges between 4 and 17 ms/km.

Time variations in ϕ and $\delta t/L$, 1996-2000

The Coso MEQ data set from 1996 to 2000 is ideal to monitor temporal variations in ϕ and $\delta t/L$. Time variations in either of these parameters may indicate changes in the dominant crack orientation, crack density or crack aspect ratio (defined as crack thickness divided by the crack diameter), all of which are of interest to monitoring production. In order to avoid seasonal variations, only events from the first six months of each year were used. The four stations selected, CE1, CE2, CE4, and CE6 are centered in the geothermal production area, have the highest number of high-quality continuous data and thus are ideal to study temporal variations in ϕ and $\delta t/L$. To minimize any preexisting bias, the data analysis is performed without any knowledge on our part of the field's production/injection operations or the location of producing wells.

Although the main polarization directions recorded at each of the four stations are highly consistent from 1996 to 2000, some temporal changes in dominant crack orientation and range of observed orientations were noted (Fig. 4).

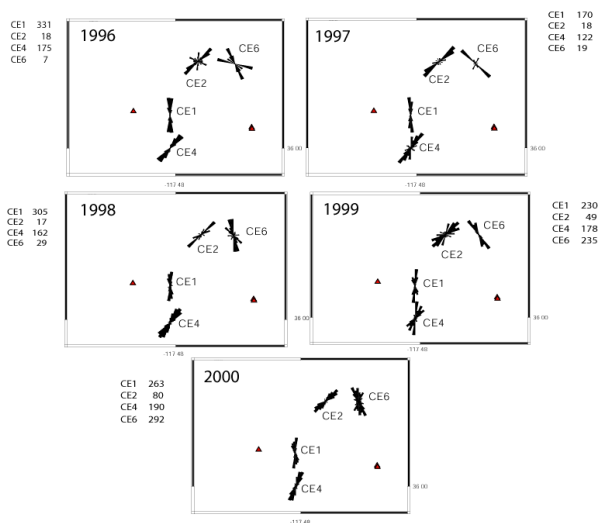


Figure 4. Rose diagrams of the observed polarizations for the central Coso stations CE1, CE2, CE4 and CE6 from 1996 to 2000. Only polarization readings with quality A to C are used.

The most significant change in dominant crack direction is observed for station CE4. In 1999 the

most prominent polarization direction at CE4 is N10E, which contrasts with the most common N30E orientation observed in previous and subsequent years. Station CE6 shows significant increase of secondary fracture orientations in the year 2000 compared to the 1999. It is important to note that station CE6 also shows large variations from 1996 to 1998, but the number of observations is much smaller, around 10% of those in 1999 and 2000. However, any of these changes could well be the result of the varying size of the sample, which depends on level of seismic activity in the shear-wave window beneath the station and may be related to production.

In 1999 there is a clear increase in the relative number of observations of the N10E polarization simultaneously at stations CE1 and CE4, which coincides with a conspicuous drop in δt at CE1, CE2, CE4 and CE6, relative to previous years (Fig. 5).

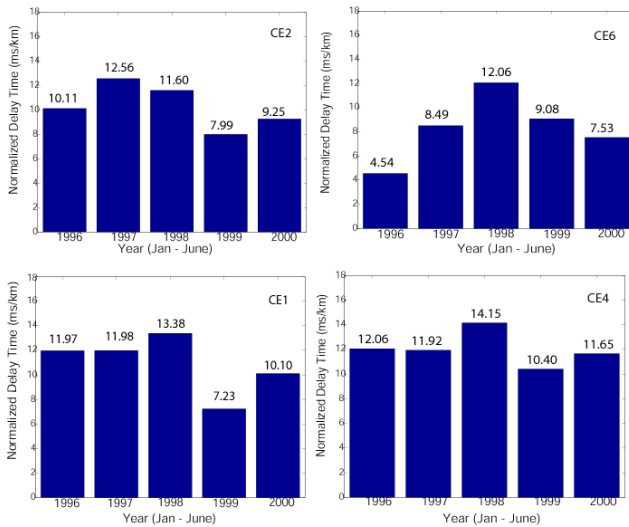


Figure 5. Mean values of the delay times per station from 1996 to 2000. Note the similarity in the histograms for stations CE2, CE1 and CE4.

Although the decrease in δt in 1999 affected all events in the shear-wave window of station CE1, the reappearance of longer time delays in 2000 was restricted to the linear zone extending approximately N10E along the center of the shear-wave window (Fig. 6; compare the graphs for 1998, 1999 and 2000). The evidence suggests that there are temporal variations in the main fracture system striking N10E underneath CE1, perhaps reaching south to CE4. The relative preeminence of the N10E polarization direction in 1999 for both CE1 and CE4 supports this hypothesis. The 1999 delay drop was less prominent at station CE6, which is also the only station that did not observe subsequent increase of time delays in the

year 2000. Concurrent evidence (which may or may not be related to the 1999 delay time drop) shows a considerable increase in seismicity recorded by the neighboring stations CE2 and CE6 starting in 1999.

Preliminary interpretation of temporal changes in δt

We used synthetic seismograms to simulate the effect of cracks along the ray path and calculate possible range of variations in elastic constants reflected in the observed 1999 drop of δt . The computation uses an elastic, anisotropic flat-layered model through which rays of designed source waves (P or S) are transmitted (e.g., Su and Park, 1994). Cracks are described in terms of their spatial orientation and the percent change in elastic constants they produce. These parameters are used to compute the synthetics for the azimuth, incidence angle and central frequency of interest. The resulting seismograms are depicted on the three components of ground motion. Simulations relevant to the Coso field observations are shown in Fig. 7. The focal depth of most events suggests use of a 1.5 km anisotropic layer over an isotropic half-space. The waves approach the receiver at near vertical incidence, and the crack orientation is assumed to be S50W (the actual orientation in the model is irrelevant for our purpose). The goal is to approximately simulate the 1999 drop in delay time observed at stations CE1, CE2 and CE4 (Fig. 5). In the model the drop in δt is equivalent to an increase in slow shear wave velocity of about 2.5%. The corresponding decrease in crack density should be of nearly the same magnitude, i.e. around 3% (e.g., Thomsen, 1995).

DISCUSSION

It is possible that the 1999 drop in the δt and N10E alignment of dominant crack directions in the CE1-CE4 region is result of episodic hydrothermal venting. The CE1-CE3-CE4 region is recognized as having the largest P-wave anisotropy (~8%) and stress concentration in the Coso geothermal field, as well as low Poisson's ratio and low porosity at the geothermal production depths from 1-1.5 km (Lees and Wu, 1999; Lees and Wu, 2000; Unruh et al, 2001). Lees and Wu (2000) proposed magmatic upwelling centered in the CE1-CE3-CE4 area and existence of highly fractured zone that serves as a major fluid conduit extending to the north (towards CE2-CE6 region) and east. Upwelling of hot fluids from the magma center through the main NNE trending fracture conduit could result in thermoelastic sealing of the secondary cracks and drop in delay times (Germanovich and Lowell, 1992). Cooling of sealed part can be followed by partial reopening of cracks by second fluid pulse, which can explain recovery of delay times only in an elongated zone

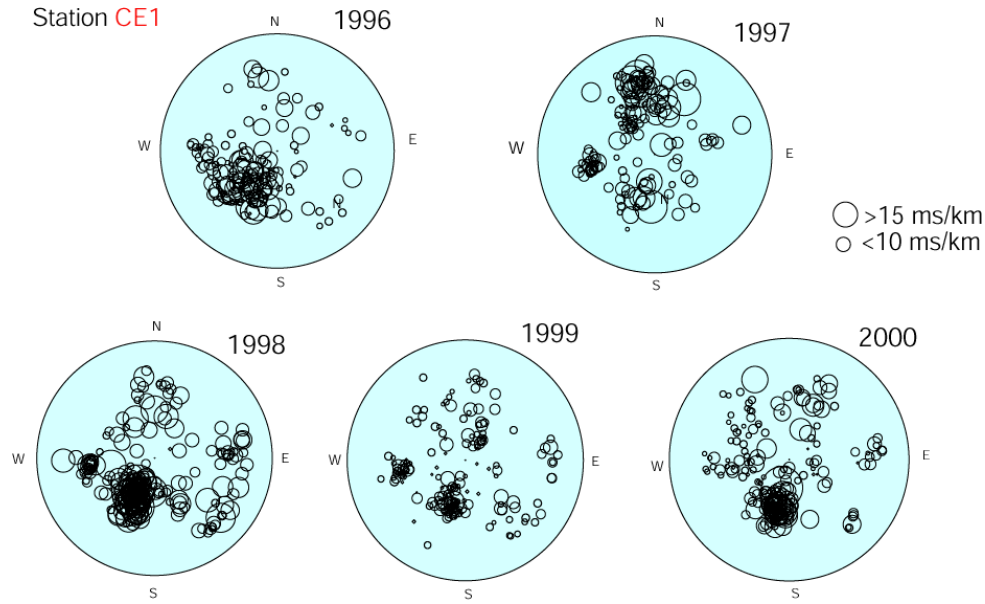


Figure 6. Equal area projections of observed time delays at the stations CE1 from 1996 to 2000. Circles show up to 45° incidence angle.

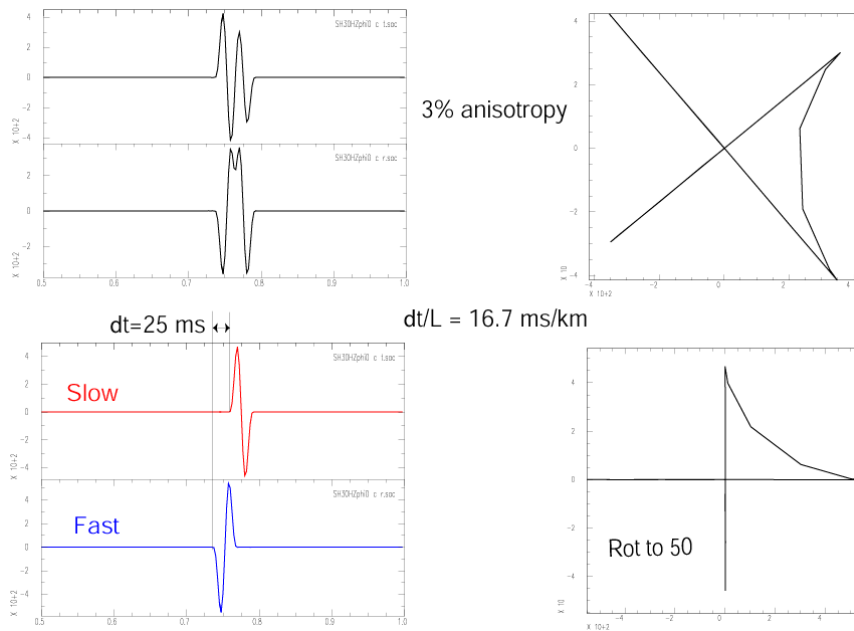


Figure 7. Synthetic seismograms simulate the drop in delay time observed in 1999. On the right diagrams the synthetic hodographs are rotated until the polarizations are parallel to the axis. This separates out the fast and slow arrivals. See details in text.

that parallels the direction of proposed fluid conduit (station CE1).

Alternatively, simultaneous drop in average delay times for stations CE1, CE2, CE4 and CE6 may be the result of stress induced changes related to the earthquake sequence that occurred on March 6, 1998. Changes in shear-wave splitting parameters have been observed before and after events ranging from $M_L = 6$ North Palm Springs, CA earthquake (Crampin et al., 1990), $M_L=4$ Parkfield, CA earthquake (Liu et al., 1993), and $M_L = 3.5$ earthquake of Enola swarm, AR (Booth et al., 1990). Bhattacharyya et al. (1999) found that effective main shock (comprised of M_L 5.2 event and three main aftershocks) produced significant stress loading of the Coso geothermal field. Stress loading of the field could result in increase of crack aspect ratios and/or increase in crack density, as stress-aligned fluid inclusions are the most responsive part of the rock mass (Crampin et al., 1990). Stress induced modifications may account for the observed increase of the average time delays in the 1998 observed at the stations CE1, CE4 and CE6. Crack healing, after relaxation of stress by the increased seismic activity that was triggered in the geothermal field following the main shock, can be very gradual. This gradual healing of the cracks may explain why time delays stayed at the elevated levels several months after the main shock. Of course, decrease of the delay times in Coso may be the final result of a number of related processes, including migration of hot fluids from the field, stresses created by injection, etc.

FUTURE WORK

Monitoring of stress changes before an impending earthquake requires swarm of small earthquakes within a shear-wave window and proximity of the seismic array to the preparation area of the larger event, conditions that are rarely present. More than five years of the high quality, three-component, continuous data recorded in the Coso geothermal field will provide us with the unique opportunity to study the possibility of using the shear-wave splitting parameters to monitor the effects of changes of strain before earthquakes. On going controlled experiment in which closely observed shear-wave splitting variations are monitored in relation to the injection/production activity in Coso, will allow us to better understand the relationship between production, tectonic stress and the observed changes in δ .

ACKNOWLEDGEMENTS

This research is supported by the US Navy Geothermal Office, Naval Air Weapons Station, contract N60530-1176-CA8R and US Department of Energy grant # DE-FG07-00ID13956. We would

like to thank Dr. Jonathan M. Lees for his valuable help.

REFERENCES

Angerer, E., Crampin, S., Li, X. -Y., 2000. Changes in shear wave anisotropy in time-lapse data: a case study, 62nd Conference EAGE, Glasgow, Extended Abstracts.

Bhattacharyya, J., Gross, S., Lees, J., Hastings, M., 1999. Recent earthquake Sequences at Coso: Evidence for Conjugate Faulting and Stress Loading near a Geothermal Field, Bulletin of the Seismological Society of America, 89, 3, 785-795.

Booth, D. C., Crampin, S., Lowell, J. H., and Chiu J. -M., 1990. Temporal Changes in Shear Wave Splitting During an Earthquake Swarm in Arkansas, Journal of Geophysical Research, 95, 7, 11,151-11,164.

Crampin, S., 1981. A review of wave motion in anisotropic and cracked elastic-media, Wave Motion, 3, 343-391.

Crampin, S., Booth, D. C., Evans, R., Peacock, S., Fletcher, J. B., 1990. Changes in Shear Wave Splitting at Anza Near the Time of the North Palm Springs Earthquake, Journal of Geophysical Research, 95, 7, 11,197-11,212.

Duffield, W.A., Bacon, C.R., 1981. Geologic map of the Coso volcanic field and adjacent areas, Inyo Co., California. USGS Map I-1200.

Feng, Q., Lees, J. M., 1998. Microseismicity, stress, and fracture in the Coso geothermal field, California, Tectonophysics, 289, 221-238.

Germanovich, L. N., Lowell, R. P., 1992. Percolation Theory, Thermoelasticity, and Discrete Hydrothermal Venting in the Earth's Crust, Science, 255, 1564-1567.

Hudson, J.A., 1981. Wave speeds and attenuation of elastic waves in material containing cracks: Geophys. J. R. Astr. Soc., 64, 133-150. 1981.

Lees, J. M., Wu, H., 1999. P wave anisotropy, stress, and crack distribution at Coso geothermal field, California, Journal of Geophysical Research, 104, 8, 17,955-17,973.

Lees, J. M., Wu, H., 2000. Poisson's ratio and porosity at Coso geothermal area, California, Journal of Volcanology and Geothermal research, 95, 157-173.

Liu, Y., Booth, D. C., Crampin, S., Evans, R., Leary, P., 1993. Shear-wave Polarizations and Possible Temporal Variations in Shear-wave Splitting at Parkfield, Canadian Journal of Exploration Geophysics, 29, 1, 380-390.

Lou, M, Rial, J. A., 1994. Characterization of the crack geometry at the Coso, California geothermal reservoir by analyzing shear-wave splitting from microearthquakes, Proceedings of the 19th Workshop on Geothermal Reservoir Engineering, Stanford, SGP-TR-147, 15-20,1994.

Lou, M., Rial, J.A., 1997. Characterization of geothermal reservoir crack patterns using shear-wave splitting, Geophysics, 62, 2, p487-495.

Roquemore, G., 1980. Structure, tectonics, and Stress Field of the Coso Range, Inyo County, California, Journal of Geophysical Research, 85, 5, 2434-2440.

Su, L., Park, J., 1994. Anisotropy and the splitting of PS waves, Physics of the Earth and Planetary Interiors, 86, 263-276.

Thomsen, L., 1995. Elastic anisotropy due to aligned cracks in porous rock. Geophysical Prospecting, 43, 805-829.

Unruh, J., Pullammanappallil, S., Honjas, W., Monastero, F., 2001. New Seismic Imaging of the Coso Geothermal Field, Eastern California, Proceedings, 26th Workshop on Geothermal Reservoir Engineering, Stanford University, Stanford, California, January 29-31, 2001, SGP-TR-168.